A Triggered Mechanism Retrieves Membrane in Seconds After Ca²⁺-stimulated Exocytosis in Single Pituitary Cells

P. Thomas, A. K. Lee, J. G. Wong, and W. Almers

Department of Physiology and Biophysics, University of Washington, Seattle, Washington 98195; and Max Planck Institut für Medizinische Forschung, Abteilung Molekulare Zellforschung, 69028 Heidelberg, Germany

Abstract. In neuroendocrine cells, cytosolic Ca²⁺ triggers exocytosis in tens of milliseconds, yet known pathways of endocytic membrane retrieval take minutes. To test for faster retrieval mechanisms, we have triggered short bursts of exocytosis by flash photolysis of caged Ca²⁺, and have tracked subsequent retrieval by measuring the plasma membrane capacitance. We find that a limited amount of membrane can be retrieved with a time constant of 4 s at 21–26°C,

and that this occurs partially via structures larger than coated vesicles. This novel mechanism may be arrested at a late step. Incomplete retrieval structures then remain on the cell surface for minutes until the consequences of a renewed increase in cytosolic [Ca²⁺] disconnect them from the cell surface in <1 s. Our results provide evidence for a rapid, triggered membrane retrieval pathway in excitable cells.

KNOWN mechanisms of endocytosis are slow (Watts and Marsh, 1992). While Ca-triggered exocytosis takes only milliseconds at synapses, and 40 ms in pituitary cells after Ca²⁺ has bound to its regulatory sites (Thomas et al., 1993*b*), retrieval of the exocytosed membrane is thought to take minutes (time constant 4 min at 23°C in chromaffin cells) (von Grafenstein et al., 1986) to hours (time constant 3 h in mast cells) (Thilo, 1985). Nonetheless, electrophysiologic measurements (Thomas et al., 1990, 1993*b*; Neher and Zucker, 1993; Tse et al., 1993) and morphologic studies on quickly frozen or fixed specimens (Knoll et al., 1991, 1992) have provided evidence for faster retrieval mechanisms after stimulated exocytosis. To explore this question, we have triggered subsecond bursts of exocytosis by photolytic release of caged Ca²⁺ into the cytosol, and have tracked membrane retrieval by measuring the electrical capacitance of the plasma membrane. The capacitance is proportional to the cell surface area, and may be used as a time-resolved assay (Neher and Marty, 1982) that can achieve millisecond resolution (Breckenridge and Almers, 1987*a*). Here we report a rapid retrieval pathway that occurs partly via vesicles of near-micron diameter. This pathway can be arrested at a late step. When the arrest was relieved by a large and sudden increase in cytosolic [Ca²⁺],

internalization was completed within a second. Evidently neuroendocrine cells can execute rapid, triggered membrane retrieval.

Materials and Methods

Melanotrophs were isolated from the pars intermedia of rat pituitaries, and maintained in culture as described (Thomas et al., 1990). Methods for recording were as described (Thomas et al., 1993 *a,b*). Briefly, cells were voltage clamped at −60 mV in the whole-cell configuration (Hamill et al., 1981) and the capacitance measured with a lock-in amplifier (Neher and Marty, 1982) using an 800-Hz, 40-mV peak-to-peak sinusoid. Besides the capacitance (90° out-of-phase component of the electrical admittance), the in-phase component was also recorded. Ca$_i$ was measured either with the Ca-indicator fura-2 or with furaptra, and was increased by flash photolysis of Ca-DM-nitrophen. DM-nitrophen and Ca-indicator entered the cell through the patch pipette; the methods of Ca$_i$ measurement and flash photolysis have been described (Thomas et al., 1993*b*). After establishing continuity between the pipette and the cytosol, we waited >120 s before attempting flash photolysis of DM-nitrophen. During this time, the entry of Ca-indicator dyes into the cytosol was monitored; sufficient dye for Ca$_i$ measurement was present already after the first 5–10 s. Less than 20 s before the flash, the phase of the lock-in amplifier was carefully set so it excluded resistive admittance changes from the capacitance trace. The tips of the glass micropipettes were large (resistances 1–2 MΩ in the extracellular recording solution) and made high-conductance connections with the cytosol (G$_s$ = 0.33 ± 0.15 μS, mean ± SD, n = 53). Consequently, changes in the pipette-cytosol conductance during an experiment were fractionally small and had negligible effect on the optimal phase setting. In the dataset of Figs. 3–5, G$_s$ = 0.48 ± 0.03 μS at the beginning of the experiments, and had changed to 0.95 ± 0.11 times that value at the ends (±SD, n = 14). Before stimulation, melanotrophs had an average membrane capacitance of 5.2 pF representing a 520 μm² surface area.

For step changes in Ca$_i$, the flash struck both the cell and the pipette, causing photolysis in both. For transient Ca$_i$ changes, the flash illuminated only the cell. The external solution contained 125 mM NaCl, 20 mM tetraethylammonium (TEA)-Cl[1], 10 mM Na-Hepes, 5.5 mM glucose, 3 mM

---

1. *Abbreviation used in this paper:* TEA, tetraethylammonium.

KCl, 2 mM $CaCl_2$ and 1 μM tetrodotoxin, pH 7.4. The solutions supplied to the cytosol through the glass micropipette are given in the figure legends. Experiments were carried out at room temperature (21-26°C); measurements are given ± standard error.

Some cells were voltage clamped with the perforated patch method (Horn and Marty, 1988). Glass micropipettes sealed against the plasma membrane contained nystatin, an ionophore that perforates the membrane patch beneath the pipette tip with ion channels. These channels pass alkali metal ions but no larger ions nor proteins, and hence connect the cytosol and pipette electrically (27 ± 9 nS SD, n = 13) without allowing their contents to mix. Nystatin (50 mg/ml) was prepared in dimethylsulfoxide and then added to the solution in the pipette to 150 μg/ml. After 15-30 min, the conductance of the connection had risen to 20 nS, and continued to rise thereafter. C_m measurements were done with a 320-Hz sinusoid. The external solution contained 115 mM NaCl, 20 mM TEA-Cl, 2 mM KCl, 10 mM Na-Hepes, 10 mM $CaCl_2$, 2 mM $MgCl_2$, 5.6 mM glucose, and 1 μM tetrodotoxin.

Results

Rapid Endocytosis in Melanotrophs

To explore the time course of membrane retrieval in single melanotrophs, we rapidly deposited new membrane on the cell surface by exocytosis, and then tracked the decline in cell surface area that followed. In Fig. 1 a, flash photolysis of Ca-DM-nitrophen, a photolabile Ca chelator, caused a step increase of cytosolic $[Ca^{2+}]$, Ca_i. Changes in cell surface area due to exo- and endocytosis were monitored by measuring the plasma membrane capacitance, C_m. Most cells responded like cell 1 (see Thomas et al., 1993b). At first, C_m increased rapidly as 0.5-1% of the cell's vesicles were released in an exocytic burst (arrow); next followed a slower phase of exocytosis probably due to vesicles that had not yet attained full exocytic competence. In cells 2 and 3, however, C_m rapidly declined following the exocytic burst and then continued to rise again. We attribute the decline in C_m to a temporary loss in cell surface area and conclude that the exocytic burst in these cells was followed by an episode of rapid membrane retrieval. Cell 3 retrieved much more membrane than the exocytic burst had added (excess retrieval), and internalized 25% of its surface in 1 s.

Although the responses of cells 2 and 3 were rare (9 of 74), rapid retrieval probably occurs regularly and fails to appear in Fig. 1 a (cell 1) only because it is masked by a large exocytic response. When Ca_i was allowed to fall again before the slower phase of exocytosis could fully develop, rapid retrieval was seen in half the cases (Fig. 1 b). Out of 38 cells, 14 showed excess endocytosis like cell 1, and 7 responded like cell 2 where C_m rose and declined to baseline. In 17 cells C_m did not decline completely, staying either constant (6 cells) or increasing in a pronounced slow phase of exocytosis (e.g., cell 3). Probably Ca_i in these cells stayed high long enough to allow some exocytosis to continue after the exocytic burst.

When the slow phase of exocytosis was inhibited by acidifying the cytosol, a rise in Ca_i triggered only a small but rapid exocytic burst (Thomas et al., 1993b), and 19 out of 21 cells responded like cells 1 or 2 in Fig. 1 b. The change in cytosolic pH had little or no effect on the time course of membrane retrieval. In Fig. 2 a, 17 responses at pH 7.2 as in Fig. 1 b (cells 1 and 2) were averaged, and compared to the average of responses at pH 6.2 selected by the same criteria (see legend). Where endocytosis is not overshadowed by exocytosis, it apparently occurs similarly at both pHs.
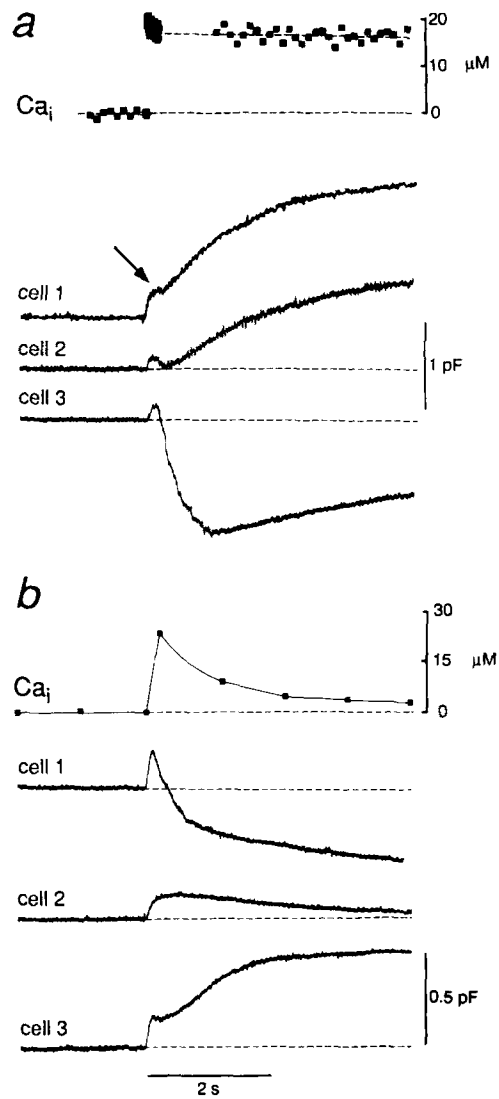

Figure 1. Surface area changes (C_m) in response to step (a) and transient changes (b) in Ca_i. The Ca_i trace in a was recorded from cell 3, that in b from cell 2. In a, the pipette contained 100 mM Cs-glutamate, 16 mM TEA-Cl, 10 mM Na_4DM-nitrophen, 8.5 mM $CaCl_2$, 2 mM NaATP, 0.1 mM furaptra, and 8 mM Cs-Hepes (pH 7.2); in b the pipette solution contained less Cs-glutamate (76 mM) and more Cs-Hepes buffer (50 mM).

Large Vesicles Contribute to the Rapid Retrieval

In cells with large secretory vesicles, exocytosis is seen to increase C_m in steps, each representing a single vesicle (Neher and Marty, 1982; Fernandez et al., 1984; Breckenridge and Almers, 1987a). This encouraged us to ask whether single membrane retrieval events can be similarly resolved (Fig. 2 c). In some cells the decline in C_m was gradual (Fig. 2 c, cell 1) but in others, it occurred in steps that were superimposed on a more gradual decline (Fig. 2 c, cells 2 and 3). To see whether the frequency of steps was correlated with the rate of membrane retrieval, we counted all steps greater than 20 fF, the smallest amplitude that is reliably detected under our conditions. With a specific membrane capacitance

Figure 3. Exocytosis and retrieval after six repeated flashes. When the pipette connected with the cytosol at $t = 0$, Ca_i transiently rose to 3 μM as Mg^{2+} displaced Ca^{2+} from the DM-nitrophen diffusing into the cell (Neher and Zucker, 1993; Thomas et al., 1993b). C_m was not recorded during the first 20 s of this experiment. Later, six flashes were given; Ca_i is off the scale during the first 10–20 s after each flash. Pipette solution as in Fig. 2, pH 6.2; Ca-indicator dye was 0.1 mM fura-2. In five cells, 0.1 mM furaptra was used instead of fura-2; flashes of the strength used here raised Ca_i to between 60 and 210 μM.
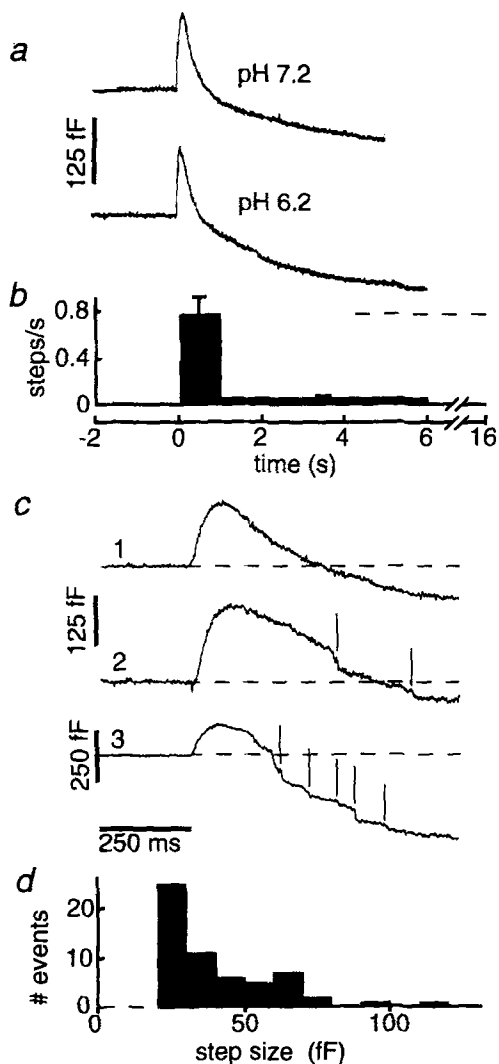

Figure 2. Stepwise membrane retrieval. (a) Averages of 17 recordings at cytosolic pH 7.2 and 18 recordings at pH 6.2. The trace at pH 7.2 is shorter because a second flash was generally given 5 s after the first. Dashed line at pH 6.2 shows the average C_m measured 16 s after the flash. Recordings were included if they satisfied all of the following: (a) C_m declined to within 20 fF of the baseline or beyond; (b) dC_m/dt remained negative throughout after C_m had reached its initial peak; and (c) second flashes were given no less than 5 s after the first. Of the 38 recordings at pH 7.2, 19 met criteria a and b, and 22 met criterion a. Of 21 recordings at pH 6.2, 19 met criteria a–c. Failure to meet a and b is attributed to contamination with a slower component of exocytosis (Fig. 1 a). Composition of solutions: pH 7.2, 76 mM Cs-glutamate, 16 mM TEA-Cl, 2 mM Na_4ATP, 50 mM Cs-Hepes buffer, 10 mM DM-nitrophen, 8.5 mM $CaCl_2$, 0.1 mM fura or furaptra; pH 6.2, as above but 7.5 mM $CaCl_2$, 50 mM Cs-MES buffer, and no ATP. (b) Frequency of downward steps of >20 fF in the recordings averaged in a. As results at pH 7.2 and 6.2 differed little, the two data sets were combined. 26 downward steps were counted in the first interval (first 1 s following peak C_m), 7 in the second (1–6 s after flash) and 1 in the third (6–16 s after flash; pH 6.2 only); the error bars shown were derived from the standard error, SE, of n, the number of steps observed in each bin (SE = $n/[n]^{1/2}$). No downward steps occurred during the 10-s intervals preceding the flash in any of the 37 cells included. (c) Initial portions of individual traces at pH 6.2 showing examples of downward steps (vertical lines); each trace from a different cell as indicated by number. The largest steps coincided with brief and transient increases in the in-phase admittance
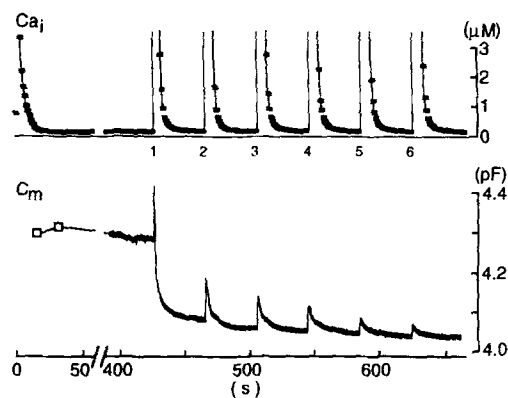
of 10 fF/μm^2, 20 fF represents a surface area of 2 μm^2, enough to surround a 0.8-μm diam vesicle. Fig. 2 b plots the frequency of steps against time for the cells analyzed in Fig. 2 a. Steps were clearly most frequent while C_m declined the fastest, i.e., during the first 1 s after an exocytic burst. However, steps also occurred later. If referred to the surface area retrieved, the difference between the first 1 s (3.7 ± 0.7 steps/pF) and next 5 s (2.3 ± 0.9 steps/pF) is no more than twofold. Evidently retrieval occurs at least partly via structures much larger than clathrin-coated vesicles (100-nm diam, expected capacitance 0.3 fF).

Nonetheless, most of the decline in C_m was not clearly stepwise. Even when steps could be resolved (Fig. 2 c), the smallest steps were the most frequent (Fig. 2 d). Evidently retrieval structures varied widely in size, and only the very largest were resolved as steps.

Excess Retrieval

At pH 6.2, repeated flash-induced Ca_i transients to 20 μM and beyond (Fig. 3) readily elicited repeated cycles of exocytosis and retrieval. Retrieval and exocytic insertion of membrane were closely matched, except that the first flash was nearly always followed by excess retrieval (16 out of 19 cells). The excess, and that it occurred only after the first flash, indicate that the cell surface had accumulated membrane marked for rapid internalization. In Fig. 3, C_m remained constant for >6 min before the first flash. Evidently mem-

(not shown, see Materials and Methods); these probably reflect the constriction and closing of the aqueous channel connecting the vesicle with the extracellular space (Rosenboom and Lindau, 1994). (d) Histogram of step sizes larger than 20 fF; the frequency of smaller steps is unknown, but expected to be large since most of the capacitance decline occurs in steps that are too small to resolve. Combined data at pH 7.2 and 6.2.

brane so marked remained on the cell surface for minutes until a flash triggered its retrieval.

Probably, the excess membrane retrieved after the first flash had been added during an earlier episode of exocytosis. Such exocytosis occurs when Ca-DM-nitrophen first enters the cell through a patch pipette. The Mg^{2+} in the cell then displaces Ca^{2+} from the chelator, and the ensuing transient rise in Ca_i (to ~3 μM at the beginning of Fig. 3) results in slow exocytosis lasting tens of seconds (Neher and Zucker, 1993; see also Fig. 7). We measured C_m <20 s after establishing continuity between cytosol and pipette, and once more after 90-120 s, just before flash photolysis of DM-nitrophen. During this time C_m grew by 258 $\pm$ 83 fF (5.6% of the cell surface, n = 16) under the conditions of Fig. 3. Excess retrieval in that group of cells was 205 $\pm$ 40 fF (5.0% of the cell surface) and tended to be largest in cells that had added the most membrane before the flash (correlation coefficient 0.43; P < 0.01). However, the correlation was not tight; one cell, for example, added >100 fF before the flash but performed no excess retrieval.

Rapid and Slower Phases of Retrieval

How fast is excess retrieval? Fig. 4 compares responses to

first and later flashes. Rate constants were measured in two ways. First, the final portions of the traces were fitted with declining exponentials, shown superimposed onto the traces as continuous lines (Fig. 4 a). Their time constants are plotted as reciprocals in Fig. 4 b (filled circles) and were constant from flash to flash. Next, initial rate constants (Fig. 4 b, open triangles) were calculated by fitting straight lines to the early portion of capacitance decline (not shown) and dividing them by the amplitude of the decline. Both measurements agreed except after the first flash, where the initial rate constant was higher. While a slower component of membrane retrieval (time constant 3.8 s) is evidently seen after each flash, there is an additional, much faster component after the first. The initial rate constant after the first flash does not fully reflect the speed of the underlying process, partly because it is the average from a data set that also includes cells without a fast phase. For a more accurate evaluation, the fast phase was separated out in Fig. 4 c, either by subtracting the exponential (upper trace) or by subtraction of the response to the second flash, scaled up in proportion to the amplitudes of the exocytic bursts (lower trace). Both methods gave similar results. In 11 cells where the fast phase had an amplitude >70 fF, the time constant was 350 $\pm$ 61 ms (subtracted exponential; Ca_i 60-210 μM).

The slower component probably retrieves the membrane added by the most recent exocytic episode, i.e., by the exocytic burst. After second and subsequent flashes, it is the only component seen, and its amplitude equals that of the preceding exocytic burst (ratio of endo- over exocytosis 1.03 $\pm$ 0.10; n = 11). Also after the first flash, slow component and exocytic burst had similar amplitudes (ratio 1.20 $\pm$ 0.09; n = 16). The slow component is less likely to show resolvable steps; in none of eight experiments did we observe steps (>20 fF amplitude) after the second flash.

In contrast, the fast phase reflects mostly excess retrieval. Like excess retrieval, it is seen only after the first flash. Cells showing no excess retrieval after the first flash also had no fast phase (Fig. 5 a). The amplitudes of both were linearly correlated (Fig. 5 b; correlation coefficient 0.90; P < 0.001); the regression line had a slope close to unity (0.81 $\pm$ 0.07
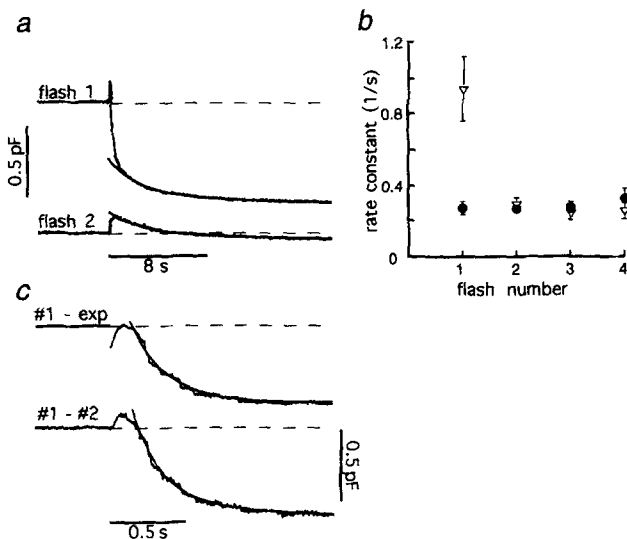
Figure 4. Two kinetic components of rapid retrieval. (a) Responses to the first two flashes. Continuous lines are the sum of a sloping baseline (fitted from 16 to 22-24 s after the flash) and a declining exponential (fitted from 1.6 to 8-10 s). (b) Rate constants of exponentials were fitted as in a (filled circles) and initial rate constants (triangles) were calculated as the steepest downward slope of the C_m trace divided by the amplitude of the decline; care was taken to include only sections of traces containing no steps (see Fig. 2 c). For each cell, the rate constant of the exponential fitted to the second flash response was taken as a reference, and all other rate constants were normalized to it. Its mean value (0.27 $\pm$ 0.03/s, n = 12) defines the ordinate. (c) Fast component after the first flash, calculated as indicated by subtracting either the fitted exponential or the response to the second flash multiplied by the ratio of the two C_m peaks (first/second). In the upper trace the initial rise in C_m reflects the exocytic burst; the pre-flash baseline was drawn at the level of the C_m peak. In the lower trace the initial C_m increase results from C_m rising faster after the first flash than after the second; the arrow marks the peak of the second flash response. Conditions same as in Fig. 3.
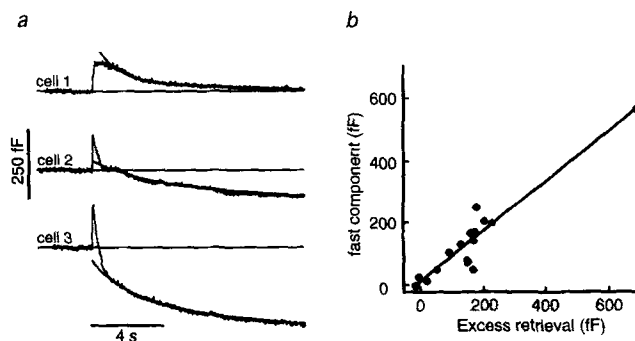

Figure 5. Correlation between excess endoctyosis and the fastest phase of retrieval. (a) First-flash recordings from three cells illustrating the range of responses seen. (b) Amplitude of the endocytic burst is the difference between peak C_m and the fitted exponential. Excess retrieval is the difference between C_m measured before and 3 τ after the flash, where τ is the time constant of the fitted exponential (mean 3.8 $\pm$ 0.4 s for first flashes, n = 18). Conditions same as in Fig. 3.

fF/fF). Probably the fast phase retrieves membrane that was left stranded on the cell surface after past exocytic episodes.

In summary, we have observed endocytosis showing two kinetic components. Even the slower of the two is much faster than the clathrin-mediated endocytosis so extensively studied in other cells. Since clathrin-mediated endocytosis probably occurs as an additional mechanism also in melanotrophs, the two kinetic components described here are collectively called rapid retrieval.

Excess Retrieval Starts with a Delay

It seemed possible that excess retrieval starts as soon as Ca^{2+} appears in the cytoplasm. To test this idea, exo- and endocytosis were considered separately in model calculations. Fig. 6 a simulates exocytosis, E, as the increase in cell surface caused by a typical exocytic burst,

$$E = B [1 - exp(-at)] \qquad (1)$$

where B is the total membrane added during the burst, a the rate constant of the burst and t the time after the flash. Fig. 6 b simulates the decrease in cell surface caused by retrieval. Retrieval, R, is assumed to occur initially linearly, $R = -rt$, and is plotted for two different rates, r (solid and dotted lines). Fig. 6 c shows the net change in surface area, ΔC:
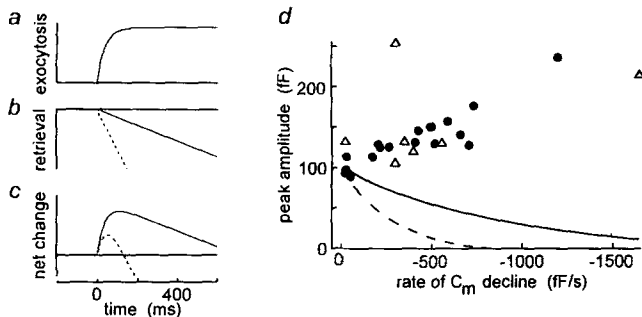

Figure 6. Effect of retrieval rate on the peak capacitance reached during the exocytic burst. (a–c) Model calculations considering exo- and endocytosis in isolation. (a) C_m change during an exocytic burst in the absence of retrieval; the curve is Eq. 1 with $a = 25/s$. (b) Retrieval is assumed to occur linearly and at two different rates. (c) Net changes in cell surface area, calculated as in Eq. 2 by adding the curve in a to each of the curves in b. (d) Calculated and observed relationships between the peak C_m increase, B_p, and the rate, r, of the C_m decline. Calculations by Eq. 3 with $B = 105 \pm 9$ fF ($n = 5$), a value based on cells where $r/a < 2$ and where, therefore, B_p underestimates B by < 10 fF when $B < 150$ fF. Assumed rate constants were $a = 27/s$ (solid line) or $8.7/s$ (dashed line). (●) Data from 17 cells as in Figs. 3–5 at saturating Ca_i; (△) data from 7 cells under conditions similar to Figs. 3–5 except that the flash caused a smaller but permanent rise in Ca_i (18 to 28 μM). For each cell, the rate of C_m decline was obtained as in Fig. 4 b by measuring the steepest downward slope of the C_m trace. The rate constant of the exocytic burst was measured as the initial rate of C_m increase divided by the the peak amplitude. Peak amplitudes and rates of C_m decline were each divided by the initial capacitance, and then multiplied by the average initial capacitance of the two data sets. This allows for a tendency for larger cells having larger burst amplitudes and, possibly, faster rates of C_m decline. Throughout, responses were included only if C_m declined to within 20 fF of the baseline or beyond.

$$\Delta C = B [1 - exp(-at)] - rt \qquad (2)$$

Clearly, the peak reached during the exocytic burst, B_p, is smaller when the rate of retrieval is larger. The relationship between the two variables B_p and r can be derived from Eq. 2:

$$B_p = B - \frac{r}{a} \left[1 + ln \left(\frac{aB}{r}\right)\right] \qquad (3)$$

In Eq. 3, B_p depends on the relative magnitudes of the rate r and the rate constant a.

Experiments as in Figs. 3–5 were analyzed to test this prediction, and Fig. 6 d plots the peak amplitude of the rise in C_m against the maximal rate at which C_m subsequently declined. While the rate of decline varied from cell to cell over a more than 50-fold range, the peak amplitude varied much less. Two data sets are compared with our model's predictions. In the first (filled circles), strong flashes raised Ca_i to 130 μM (range 60–210 μM) and stimulated exocytic bursts with an average rate constant of $27 \pm 2/s$ ($n = 17$, see legend), the maximum reached at saturating Ca_i (Thomas et al., 1993b). For this rate constant, the model predicts the continuous line in Fig. 6 d. In the other data set, weaker flashes caused smaller rises in Ca_i (to 20 μM, range 18 and 28 μM) and triggered slower exocytic bursts (rate constant 8.7 ± 1.4, $n = 7$). The model predicts the dashed line.

The data are inconsistent with the model in two ways. First, peak amplitudes were no larger for the faster (133 $\pm$ 8 fF, $n = 17$) than the slower exocytic bursts (155 $\pm$ 21 fF, $n = 7$); this is contrary to Eq. 3. When peak amplitudes of exocytic bursts were plotted against their rate constants (not shown), the regression line had a slope of -1.3 ± 0.7 fF s with no correlation between the two variables (correlation coefficient $r^2 = 0.12$, $n = 26$, $P > 0.95$). Second and more strikingly, in neither data set did peak amplitude diminish with increasing retrieval rate. This is seen also in Fig. 5 a, where the cell with the slowest retrieval (cell 1) had a response no larger than two cells with much faster retrieval (cells 2 and 3). Instead there was a tendency for retrieval to be fastest after the largest exocytic bursts, as if the two events were co-regulated, or as if a substance required for rapid retrieval were released in proportion to the exocytic burst. Model and data might yet be reconciled if cells with faster retrieval also had exocytic bursts with proportionately faster rate constants. However the two variables were uncorrelated ($r^2 = 0.05$, $P > 0.95$, $n = 25$). Clearly, retrieval does not diminish the peak capacitance reached during the exocytic burst. Evidently no significant retrieval occurs during the burst, hence retrieval must start with a delay lasting about as long as the burst.

Only a Limited Amount of Membrane Is Retrieved Rapidly

In Fig. 3, membrane retrieval was complete even after repeated flashes. This is because at cytosolic pH = 6.2 relatively little exocytosis takes place; even after six repeated flashes, cumulative exocytosis is only 384 ± 16 fF ($n = 9$). At pH = 7.2, in contrast, a step rise in Ca_i elicits an exocytic burst followed by a slower but larger exocytic phase of $\sim$1 pF amplitude (Fig. 1 a, cell 1) (Thomas et al., 1993b),
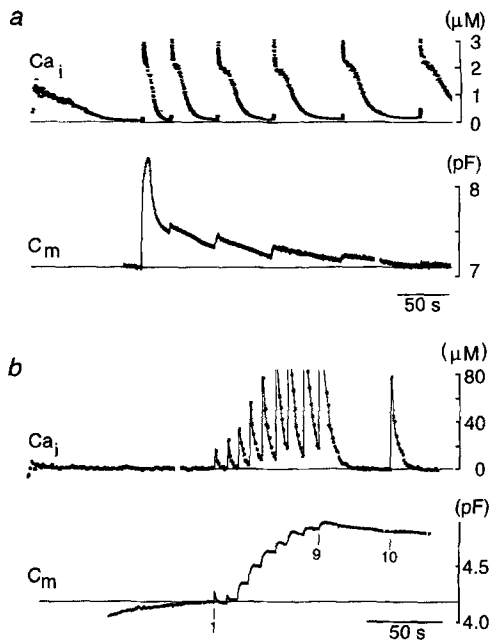
Figure 7. Massive exocytosis exhausts the rapid retrieval mechanism. (*a*) Same as in Fig. 3 but with cytosolic pH = 7.2 (pipette solution as in Fig. 1 *a*). Ca_i was measured with 0.1 mM fura-2, and was therefore off the scale for the first few seconds after each flash. In this cell, the first flash caused massive exocytosis, possibly because Ca_i did not fall rapidly enough to prevent a large, slower phase of exocytosis (compare Fig. 1 *b*, cell *3*) described elsewhere (Thomas et al., 1993*b*). (*b*) Response to 9 rapidly repeating flashes in another cell, where the first flashes caused only moderate rises in Ca_i. Ca_i measured with 0.1 mM furaptra, a Ca^{2+} indicator of lower affinity. Pipette solution same as in Fig. 1 *b*. Note slow C_m increase before the flash; membrane exocytosed during that time may contribute to excess retrieval. Throughout, the Ca_i trace starts when the pipette first connects to the cytosol.

and this slower phase of exocytosis is sometimes seen also during a transient rise in Ca_i (Fig. 1 *b*, cell 3). Once Ca_i had fallen and exocytosis had stopped in such cases (Fig. 7 *a*), endocytosis at a speed comparable to the slower component in Figs. 3–5 was seen, but only about half the added membrane was retrieved at that speed. The remainder was retrieved in an ultraslow phase that continued when the second and subsequent flashes brought additional exocytosis. In three cells the first flash raised C_m by more than 1 pF (>17% of the cell surface); these cells retrieved only ∼0.5 pF (7.3 ± 2.0% of cell surface) within 10 s after C_m had reached a peak. Evidently the rapid retrieval mechanisms studied here have a limited capacity.

In Fig. 7 *b*, the flashes repeated so rapidly that Ca_i could not decline completely during the intervals, and instead summed from flash to flash. After the first two flashes, Ca_i fell sufficiently before the slower phase of exocytosis could occur, and retrieval was seen to occur at a rate similar to that of the slower component in Figs. 3–5. After later flashes, however, any such retrieval was masked by exocytosis. Ultimately, it was abolished altogether, because when Ca_i was allowed to decline to levels too low to support exocytosis, C_m declined at a rate that was barely measurable (8.5 ± 2.9 fF/s, *n* = 24). At that rate, the 1.3 ± 0.1 pF (*n* = 36) added in such experiments would be retrieved with a rate constant of 0.7%/s, or a time constant of 150 s. This is similar to the

much slower endocytosis measured with extracellular marker in chromaffin cells (time constant 222 s at 23°C) (von Grafenstein et al., 1986). When Ca_i rose again after a final flash, it neither caused exocytosis nor did it hasten membrane retrieval. Under our conditions of a Mg^{2+}-free cytosol, strong stimulation evidently exhausts a cell's capacity for both exocytosis and rapid retrieval, but retrieval is exhausted first. The effect cannot reflect the escape of a soluble cytosolic mediator into the pipette (washout). While vigorous retrieval still occurred 430 s after pipette and cytosol became continuous (Fig. 3), stimulation caused exhaustion within only 50 s in Fig. 7 *a*.

Rapid Retrieval in Intact Cells

To study retrieval under more physiologic conditions, we recorded from cells through perforated patches that create an electrical connection between micropipette and cytosol without allowing their contents to mix. Since DM-nitrophen cannot pass through the perforated patch, Ca_i was raised by making the plasma membrane voltage positive and opening voltage-gated Ca channels. Cells were kept at 30–32°C to increase Ca influx and exocytosis (Thomas et al., 1990).

In Fig. 8, three voltage pulses were applied to the plasma membrane to open Ca channels and raise Ca_i. Three times C_m rose and declined. In half the cases (7 of 13 cells) C_m declined to the baseline, occasionally even beyond it. The time constant of decline (4.6 ± 0.9 s, *n* = 15) was similar to that of the exponentials fitted in flash photolysis experiments Figs. 4 *a* and 5 *a* (21–26°C), though, given the higher temperature, it must be considered to be somewhat slower. In the other six cells, the decline of C_m was incomplete; if these cells are included, membrane retrieval was 90% complete in 20–30 s (35 trials on 13 cells). We conclude that the retrieval mechanism operating after flash photolysis also operates under more physiologic conditions.

Figure 8. Membrane retrieval in intact cells. Three 200-ms long voltage pulses transiently stepped the plasma membrane potential from −60 mV to 20 mV; each opened voltage-gated Ca channels, transiently raised Ca_i, and caused episodes of exo- and endocytosis. Ca_i is unknown because the cytosol contained no Ca-indicator. Since no tetraethylammonium[+] was present internally, Ca-activated K channels caused large conductance increases; the C_m trace was blanked out while the conductance declined to 100–200 nS but is considered reliable thereafter. For analysis, a straight line was fitted to the 10-s segment preceding each voltage pulse (*dashed*) and taken as a baseline for the later rise and fall of C_m. For each cell, we analyzed the first three trials that resulted in a C_m change greater than 50 fF. The pipette contained 135 mM Cs-glutamate, 20 mM TEA-glutamate, 5 mM $MgCl_2$, 2 mM Na_4ATP, 0.4 mM Li_4GTP, 150 μg/ml nystatin, and 10 mM Cs-Hepes, pH 7.3. The cytosol is expected to gain Cs^+ and lose Na^+ and K^+, but other changes are expected to be minimal. Temperature 30–32°C.

Discussion

When cytosolic $[Ca^{2+}]$ rises above 20 μM, it triggers in neuroendocrine (Neher and Zucker, 1993; Thomas et al., 1993a,b) and mast cells (Kirillova et al., 1993) an exocytic burst that runs its course in a fraction of a second. Here we provide evidence for a retrieval mechanism that can re-internalize nearly all the exocytosed membrane within 10 s. The mechanism has limited capacity (generally <1 pF or <20% of the cell surface area), and is exhausted by massive exocytosis. It is prominent in melanotrophs under physiologic conditions where exocytosis is rarely exhaustive; its probable action may be recognized also in recordings from chromaffin cells stimulated by plasma membrane depolarization (Neher and Marty, 1982) and from gonadotrophs secreting rhythmically in response to gonadotropin-releasing hormone (Tse et al., 1993).

Though uncharacterized morphologically, the structures used by this mechanism are unlikely to be clathrin-coated vesicles. First, retrieval continues vigorously under conditions that block clathrin-mediated endocytosis in other cells, namely lack of cytosolic K^+ (Larkin et al., 1985) and low cytosolic pH (Davoust et al., 1987; Sandvig et al., 1987; Heuser, 1989). Second, some of the rapid retrieval occurs in steps indicating retrieval structures of >0.8-μm diam, much larger than the 100-nm diam clathrin-coated vesicles. Lastly, even the slower of the two kinetic components retrieves membrane with a time constant of ~4 s (21–26°C); much faster than any measurement of clathrin-mediated endocyosis that we are aware of. The fastest probably clathrin-mediated endocytosis occurs at neuronal synapses with a time constant (τ) of tens of seconds (Miller and Heuser, 1984). BHK cells internalize bound Semliki forest virus via coated pits; 60% of the bound virus is internalized in 30 min at 37°C, corresponding to $\tau = 33$ min (Marsh and Helenius, 1980). In chromaffin cells, coated vesicles retrieve exocytosed membrane with $\tau = 15$ min at 37°C (Patzak et al., 1987); if measured with extracellular markers, retrieval happens with $\tau = 4$ min at 23°C (von Grafenstein et al., 1986), possibly via coated vesicles. The retrieval observed here is faster also in absolute terms. BHK cells internalize 1–2%/s of their surface area at 37°C (Marsh and Helenius, 1980). After an exocytic burst in melanotrophs, the faster of the two components retrieves membrane at an average initial rate of 600 fF/s or 12% surface area per second.

In a variety of cells there is evidence for retrieval mechanisms other than, and operating in parallel with, clathrin-mediated endocytosis (reviewed by van Deurs et al., 1989; Watts and Marsh, 1992). In motor nerve terminals, so-called vacuoles appear within the first few seconds after stimulation and differ from coated vesicles by their content of intramembrane particles (Miller and Heuser, 1983). So-called vacuoles also form in neuroendocrine cells, where they are as large as (and occasionally larger than) dense core secretory vesicles, and readily fill with extracellular marker (chromaffin cells; Baker and Knight, 1981; posterior pituitary nerve endings, Nordmann and Artault, 1992; melanotrophs, Bäck et al., 1993). In single posterior pituitary nerve terminals, such vacuoles were observed to form at a rate of 0.4–0.7/s during the first 0.5 s after a stimulus, and at only 0.03–0.13/s during the next 5 s (Knoll et al. 1992). If the rate of vacuole formation in this work was proportional to the amount of membrane awaiting retrieval, then this retrieval proceeded with a time constant of 1–1.5 s (37°C). We suggest that the retrieval seen here occurs similarly, that the vacuoles retrieved vary in size and that the very largest were detected as steps. The steps indicate structures (>0.8-μm diam) larger than the largest secretory vesicles (0.3-μm diam in rat melanotrophs) (Bäck, 1992).

Excess Retrieval Is a Triggered Event

When exocytosis was caused by the smaller Ca_i increases (1–5 μM) occurring when the Ca-DM-nitrophen entered the cell (loading transients), C_m rose slowly but did not decline (e.g., Fig. 7). Evidently, the retrieval mechanism studied here caused no, or incomplete, retrieval in this case. However, when a later and larger rise in Ca_i triggered an exocytic burst, retrieval was vigorous, had two kinetic components, and exceeded the membrane deposited by the exocytic burst. In all likelihood, the excess retrieval removes membrane that had been added during the loading transient. (a) Once triggered by a first flash, excess retrieval failed to appear again after subsequent flashes; (b) the excess was similar in magnitude to the exocytosis recorded before the first flash; and (c) it tended to be largest in cells that had added the most membrane before the flash. Excess retrieval after flash photolysis of DM-nitrophen was seen also in chromaffin cells (Neher and Zucker, 1993); there, too, exocytosis had occurred previously and the added membrane had escaped endocytosis. We suggest that the fastest retrieval component seen here internalized membrane that had accumulated on the cell surface during previous exocytic episodes. This retrieval may be termed triggered in that it is temporally correlated with the flash and not with the event that had added the membrane originally.

The added membrane and its resident proteins are insufficient as a trigger, because otherwise no such membrane could accumulate. The trigger could be an agent liberated during the exocytic burst; this could explain why excess retrieval starts with a delay. Alternatively, it could be the high Ca_i triggering the burst. At the motor nerve terminal, endocytosis requires Ca^{2+} since exocytosis stimulated by α-latrotoxin causes depletion of vesicles when Ca^{2+} is lacking (Cecarelli and Hurlbut, 1980). In rat mast cells where a rise in Ca_i alone fails to trigger exocytosis, micromolar Ca^{2+} was shown to stimulate retrieval independently of exocytosis (Almers and Neher, 1987). In previous work on melanotrophs, however, retrieval was not clearly Ca_i sensitive in the micromolar range (Thomas et al., 1990). Regulation of endocytosis was observed also in A431 cells where epidermal growth factor stimulates macropinocytosis via large vacuoles (Haigler et al., 1979; West et al., 1989).

Excess retrieval is clearly related to the fastest of the two kinetic components seen here, and is the fastest membrane internalization event that we are aware of ($\tau = 350$ ms at 21–26°C). Its speed suggests to us that preparations for this event had started well before the flash, but had become arrested at a late step. An example for genetic arrest at a late step of membrane retrieval is the *shibire* mutant of *Drosophila*, where clathrin-coated vesicles form but fail to pinch off the plasma membrane (Kosaka and Ikeda, 1983). This phenotype results from a defect in the protein dynamin (Chen et al., 1991; Van der Blick and Meyerowitz, 1991).
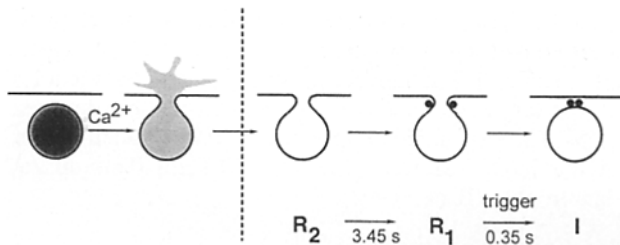
Figure 9. Proposed origin of the two kinetic components of rapid retrieval. Exocytosis leads to retrieval vesicles (R_2) that are similar in size to secretory vesicles, possibly because they *are* the empty secretory vesicles. It is proposed to take 3.45 s to prime or generate the machinery (*black dots*) for pinching off the vesicle from the plasma membrane. At this point (R_1), retrieval may be arrested for minutes. During that time, some of the vesicles may coalesce into larger structures that cause downward capacitance steps. Completion of retrieval is initiated by an unknown mediator (possibly [Ca^{2+}] >20 μM) that takes effect after a short delay ($\sim$100 ms, not shown) and causes the fastest phase of retrieval (time constant 0.35 ms). The membrane deposited during an exocytic burst is retrieved without arrest and with a time constant of $3.45 + 0.35 = 3.8$ s.

Assuming that the two kinetic phases of rapid retrieval represent the same pathway, we suggest that they represent late and early steps. In Fig. 9, Ca-induced exocytosis and membrane retrieval are shown schematically. R_2 and R_1 represent different stations along the retrieval pathway, and I is the internalized vesicle after it has disconnected from the cell surface. We propose that the reactions R_2–R_1 are normally rate limiting after an exocytic burst, so that retrieval occurs with an overall time constant of $3.45 + 0.35 = 3.8$ s. Under some conditions, however, retrieval is arrested at R_1, possibly because a substance needed for a final retrieval step is lacking. We suggest that this is the case after the loading transient at the start of an experiment has caused slow exocytosis. Retrieval structures then accumulate, and some may coalesce to form large vesicles that cause stepwise capacitance changes. When the trigger appears during the exocytic burst, the retrieval vesicles disconnect from the plasma membrane in 0.35 s. Because excess endocytosis starts after a delay about as long as the exoctyic burst ($\sim$100 ms), we must assume either that trigger does not appear instantly after a rise in Ca_i, or that a sequence of reactions is required before accumulated vesicles disconnect from the cell surface.

Speed Enhances the Selectivity of Retrieval

The exposure of vesicle antigens on the cell surface of chromaffin cells for up to 45 min (e.g., Patzak et al., 1987) shows that some vesicles completely flatten out into the plasma membrane after exocytosis, and that their membrane is retrieved only slowly. Nonetheless, it seems possible that many (and, under our conditions most) secretory vesicles fuse and release their contents without flattening out into the plasma membrane. Instead they may remain connected by an aqueous channel that is closed again a few seconds after exocytosis (Fig. 9). This was suggested for synaptic vesicles at the vertebrate motor nerve terminal (Meldolesi and Ceccarelli, 1981), and applies also to *Paramecium*, where the exocytic opening of the trichocyst cavity closes <0.35 s after exocytic expulsion of the trichocyst (Knoll et al., 1991). It

is tempting to suggest that a similar mechanism operates in neuroendocrine cells: (*a*) retrieval is fast; (*b*) except for the excess after a first flash, retrieval is closely matched to exocytosis; and (*c*) retrieval vesicles of the same size as secretory vesicles are seen morphologically. Furthermore, in mast cells where exocytosis of single secretory vesicles can be observed as stepwise increases in C_m, secretory vesicles open reversibly to the extracellular space (Fernandez et al., 1984; Spruce et al., 1990) and close before having released all their contents (Breckenridge and Almers, 1987*b*; Alvarez de Toledo et al., 1993).

Such a mechanism would need no molecular recognition to selectively retrieve exocytosed membrane proteins. Assume a 210-nm vesicle connected through exocytosis to the plasma membrane of a 15-μm diam neuroendocrine cell by a 42-nm diam neck (see Schmidt et al., 1983) that is infinitesimally short. Except for a scaling factor, this geometry corresponds to one solved by Rubin and Chen (1990; their Fig. 2 *b*) in the context of membrane mixing after the fusion of a viral envelope with the cell membrane. For proteins moving in the plane of the membrane with a typical diffusion coefficient of 0.01–0.001 μm^2/s (Jacobson et al., 1987), Rubin and Chen's model predicts equilibration with time constants of 40–400 s, 10–100 times longer than the average time such a vesicle stays connected to the cell surface. For proteins, this retrieval mechanism would be selective simply because the bilayers of vesicle and plasma membrane do not remain connected long enough for their proteins to mix extensively. By contrast, lipids diffusing at a typical 1 μm^2/s would equilibrate completely (time constant 0.4 s).

References

Almers, W., and E. Neher. 1987. Gradual and stepwise changes in the membrane capacitance of rat peritoneal mast cells. *J. Physiol. (Lond.).* 386:205–217.

Alvarez de Toledo, G., R. Fernandez.-Chacon, and J. M. Fernandez. 1993. Release of secretory products during transient vesicle fusion. *Nature (Lond.).* 363:554–557.

Bäck, N. 1992. The effect of bromocriptine on the intermediate lobe of the rat pituitary: an electron-microscopic, morphometric study. *Cell Tissue Res.* 255:405–410.

Bäck, N., S. Soinila, and I. Virtanen. 1993. Endocytotic pathways in the melanotroph of the rat pituitary. *Histochem. J.* 25:133–139.

Baker, P. F., and D. E. Knight. 1981. Calcium control of exocytosis and endocytosis in bovine adrenal medullary cells. *Philos. Trans. R. Soc. Lond. Ser. B Biol. Sci.* 296:83–103.

Breckenridge, L. J., and W. Almers. 1987*a*. Currents through the fusion pore that forms during exocytosis of a secretory vesicle. *Nature (Lond.).* 328:814–817.

Breckenridge, L. J., and W. Almers, 1987*b*. Final steps in exocytosis observed in a cell with giant secretory granules. *Proc. Natl. Acad. Sci. USA.* 84:1945–1949.

Ceccarelli, B., and W. P. Hurlbut. 1980. Ca-dependent recycling of synaptic vesicles at the frog neuromuscular junction. *J. Cell Biol.* 87:297–303.

Chen, M. S., R. A. Obar, C. C. Schroeder, T. W. Austin, C. A. Poodry, S. C. Wadsworth, and R. B. Vallee. 1991. Multiple forms of dynamin are encoded by *shibire*, a *Drosophila* gene involved in endocytosis. *Nature (Lond.).* 361:583–586.

Davoust, J., J. Gruenberg, and K. E. Howell. 1987. Two threshold values of low pH block endocytosis at different stages. *EMBO (Eur. Mol. Biol. Organ.) J.* 6:3601–3609.

van Deurs, B., O. W. Petersen, S. Olsnes, and K. Sandvig. 1989. The ways

of endocytosis. *Int. Rev. Cytol.* 117:131–175.

Fernandez, J. M., E. Neher, and B. T. Gomperts. 1984. Capacitance measurements reveal stepwise fusion events in degranulating mast cells. *Nature (Lond.).* 312:453–455.

von Grafenstein, H., C. S. Roberts, and P. F. Baker. 1986. Kinetic analysis of the triggered exocytosis/endocytosis secretory cycle in cultured bovine adrenal medullary cells. *J. Cell Biol.* 103:2343–2352.

Haigler, H. T., J. A. McKanna, and S. Cohen. 1979. Direct visualization of the binding and internalization of epidermal growth factor in human carcinoma cells A431. *J. Cell Biol.* 81:383–395.

Hamill, O. P., A. Marty, E. Neher, B. Sakmann, and F. J. Sigworth. 1981. Improved patch-clamp techniques for high resolution current recording from cells and cell-free membrane patches. *Pfluegers Arch. Eur. J. Physiol.* 391:85–100.

Heuser, J. E. 1989. Effects of cytoplasmic acidification on clathrin lattice morphology. *J. Cell Biol.* 108:401–411.

Horn, R., and A. Marty. 1988. Muscarinic activation of ionic currents measured by a new whole-cell recording method. *J. Gen. Physiol.* 42:145–159.

Jacobson, K., A. Ishihara, and R. Inman. 1987. Lateral diffusion of proteins in membranes. *Annu. Rev. Physiol.* 49:163–175.

Kirillova, J., P. Thomas, and W. Almers. 1993. Two independently regulated secretory pathways in mast cells. *J. Physiol. (Paris).* 87:203–208.

Knoll, G., C. Braun, and H. Plattner. 1991. Quenched flow analysis of exocytosis in *Paramecium* cells: time course, changes in membrane structure, and calcium requirements revealed after rapid mixing and rapid freezing of intact cells. *J. Cell Biol.* 113:1295–1304.

Knoll, G., H. Plattner, and J. J. Nordmann. 1992. Exo-endocytosis in isolated peptidergic nerve terminals occurs in the subsecond range. *Biosci. Rep.* 12:495–501.

Kosaka, T., and Ikeda, K. 1983. Reversible blockage of membrane retrieval and endocytosis in the garland cell of the temperature-sensitive mutant of *Drosophila melanogaster, shibire*. *J. Cell Biol.* 97:499–507.

Larkin, J. M., M. S. Brown, J. L. Goldstein, and R. G. W. Anderson. 1983. Depletion of intracellular potassium arrests coated pit formation and receptor-mediated endocytosis in fibroblasts. *Cell.* 33:273–285.

Marsh, M., and A. Helenius. 1980. Adsorptive endocytosis of semliki forest virus. *J. Mol. Biol.* 142:439–454.

Meldolesi, J., and B. Ceccarelli. 1981. Exocytosis and membrane recycling. *Philos. Trans. R. Soc. Lond. Ser. B. Biol. Sci.* 296:55–65.

Miller, T. M., and J. E. Heuser. 1984. Endocytosis of synaptic vesicle membrane at the frog neuromuscular junction. *J. Cell Biol.* 98:685–698.

Neher, E., and A. Marty. 1982. Discrete changes of cell membrane capacitance observed under conditions of enhanced secretion in bovine adrenal chromaffin cells. *Proc. Natl. Acad. Sci. USA.* 79:6712–6716.

Neher, E., and E. S. Zucker. 1993. Ca²⁺-dependent steps in chromaffin cell

secretion. *Neuron.* 10:21–30.

Nordmann, J. J., and J.-C. Artault. 1992. Membrane retrieval following exocytosis in isolated neurosecretory nerve endings. *Neuroscience.* 49:201–207.

Patzak, A., D. Aunis, and K. Langley. 1987. Membrane recycling after exocytosis: an ultrastructural study of cultured chromaffin cells. *Exp. Cell Res.* 171:346–356.

Rosenboom, H., and M. Lindau. 1994. Exo-endocytosis and closing of the fission pore during endocytosis in single pituitary nerve terminals internally perfused with high calcium concentrations. *Proc. Natl. Acad. Sci. USA.* In press.

Rubin, R. J., and Y. Chen. 1990. Diffusion and redistribution of lipid-like molecules between membranes in virus–cell and cell–cell fusion systems. *Biophys. J.* 58:1157–1167.

Sandvig, K., S. Olsnes, O. W. Petersen, and B. van Deurs. 1987. Acidification of the cytosol inhibits endocytosis from coated pits. *J. Cell Biol.* 105:679–689.

Schmidt, W., A. Patzak, G. Lingg, and H. Winkler. 1983. Membrane events in adrenal chrommaffin cells during exocytosis: a freeze-etching analysis after rapid cryofixation. *Eur. J. Cell Biol.* 32:31–37.

Spruce, A. E., L. J. Breckenridge, A. K. Lee, and W. Almers. 1990. Properties of the fusion pore that forms during exocytosis of a mast cell secretory vesicle. *Neuron.* 4:643–654.

Thilo, L. 1985. Selective internalization of granule membrane after secretion in mast cells. *Proc. Natl. Acad. Sci. USA.* 82:1711–1715.

Thomas, P., A. Surprenant, and W. Almers. 1990. Cytosolic Ca²⁺, exocytosis and endocytosis in single melanotrophs of the rat pituitary. *Neuron.* 5:723–733.

Thomas, P., J. G. Wong, and W. Almers. 1993a. Millisecond studies of secretion in single rat pituitary cells stimulated by flash photolysis of caged Ca²⁺. *EMBO (Eur. Mol. Biol. Organ.) J.* 12:303–306.

Thomas, P., J. G. Wong, A. K. Lee, and W. Almers. 1993b. A low affinity Ca²⁺ receptor controls the final steps in peptide secretion from pituitary melanotrophs. *Neuron.* 11:93–104.

Tse, A., F. W. Tse, W. Almers, and B. Hille. 1993. Rhythmic exocytosis stimulated by GnRH-induced calcium oscillations in rat gonadotropes. *Science (Wash. DC).* 260:82–84.

Van der Blick, A. M., and E. M. Meyerowitz. 1991. Dynamin-like protein encoded by the *Drosophila shibire* gene associated with vesicular traffic. *Nature (Lond.).* 351:411–414.

Watts, C., and M. Marsh. 1992. Endocytosis: what goes in and how? *J. Cell Sci.* 103:1–8.

West, M. A., M. S. Bretscher, and C. Watts. 1989. Distinct endocytic pathways in epidermal growth factor-stimulated human carcinoma A431 cells. *J. Cell Biol.* 109:2731–2739.